RSC Advances

PAPER

View Article Online
View Journal | View Issue

Cite this: *RSC Adv.*, 2025, **15**, 49728

Au-modified ZnO thin films for higher-performance ultraviolet photodetectors

Akshta Rajan,[a] Kashima Arora,[b] Bhavna Vidhani,[c] Jasvir Dalal *[a] and Pawan Kumar[d]

Received 25th October 2025
Accepted 8th December 2025

DOI: 10.1039/d5ra08186f

rsc.li/rsc-advances

ZnO-based ultraviolet (UV) photodetectors are widely studied due to their wide bandgap and higher photosensitivity. However, the ZnO thin-film UV photodetectors face higher dark current and limited gain despite their wide bandgap advantage. Here, Au overlayers (5–40 nm) were deposited on optimized 221 nm ZnO (prepared *via* sol–gel method) films using cost-effective spin-coating (ZnO film) and RF sputtering (Au overlayers). Au induces Schottky barriers (ϕ_{Au} = 5.47 eV > ϕ_{ZnO} = 4.45 eV) that suppress dark current down to 7.29 nA. Meanwhile, plasmonic Au nanoparticles generate localized surface plasmon resonance (LSPR) hot electrons that enhance UV absorption and photocurrent. The device with a 10 nm Au overlayer achieves an excellent photoresponse of 7.79 × 10^3 and a photocurrent of 50 μA under ultra-low 24 μW cm^{-2} UV illumination (365 nm). This performance surpasses literature values at lower UV intensity, also among the highest reported for ZnO detectors prepared using the sol–gel method. The optimized Au–ZnO devices also exhibit fast response (T_r = 15 s) and scalable fabrication routes. These results reveal the promise of Au/ZnO hybrid thin films for sensitive, lower-intensity UV detection with applications in flame sensing, wearable optoelectronics, and environmental monitoring.

1. Introduction

Ultraviolet (UV) photodetection is vital for environmental monitoring, flame sensing, wearable electronics, and security applications due to the distinct signatures of UV radiation.[1–3] Among various semiconductor materials, ZnO has garnered significant interest as a UV photodetector candidate for its wide direct bandgap (~3.37 eV), higher exciton binding energy, and chemical stability.[4] However, ZnO-based devices still struggle with higher dark current and relatively lower photocurrent-to-dark current (I_{on}/I_{off}) ratios, limiting their practical sensitivity and energy efficiency.[5,6] Recent research on ZnO-based UV photodetectors has focused on attaining high I_{on}/I_{off} ratios and shorter rise and fall times (T_r and T_f).[7,8] These performance metrics can be substantially improved through the incorporation of metals either on the surface or within the bulk of the ZnO detection layer.[9–12] Metals can be deposited as nanostructured overlayers of controlled thickness and morphology or introduced into the ZnO lattice as dopants to tailor the defect profile. Incorporation of metals such as Mg,[13] Al,[14] Cu, Li,[15] Ga,[16] Sn, Cr, Te,[17] Au,[18] Pt,[19] and Ti[20] in forms including dopants, nanoparticles, and overlayers has been reported to alter the structural, optical, and electrical properties of ZnO, thereby enhancing photodetector performance. For example, Ga doping has been employed to generate localized defect states at lattice discontinuities, improving response speed,[21] while Cu and Li doping has been shown to introduce acceptor states *via* Cu^+ ions and Li_i or Li_{Zn}–Li_i complexes, increasing film resistivity and reducing dark current.[15]

Noble metals such as Ag, Au, and Pt possess unique structural, optical, and electronic properties that make them attractive modifiers for ZnO.[22] Their ionic radii Ag^{2+} (1.2 Å), Au^{2+} (0.9 Å), and Pt^{2+} (0.9 Å) are comparable to that of Zn^{2+} (0.74 Å),[21,26] enabling potential lattice incorporation. Their work functions ϕ_{Au} = 5.47 eV, ϕ_{Ag} = 4.74 eV, and ϕ_{Pt} = 5.93 eV are higher than that of ZnO (ϕ_{ZnO} = 4.45 eV),[27,28] facilitating Schottky barrier formation at the metal–ZnO interface, which is known to suppress dark current. Furthermore, in nanoparticulate form, these metals (Ag, Au, and Pt) exhibit localized surface plasmon resonance (LSPR), enabling strong light–matter interactions when their size is smaller than the incident wavelength.[29,30] Although such plasmonic properties have been extensively exploited in photovoltaic and photonic devices, their application to enhancing UV photon absorption in ZnO photodetectors remains limited.[23] Oxygen affinity further influences device performance; Pt is overpriced and Ag exhibits higher oxygen affinity, readily forming silver oxides that can increase dark current.[31] Consequently, Au is identified as optimal choices due to their stability, lower oxygen reactivity, and ability to suppress dark current while enhancing photocurrent.[24] Thus, the integration of Au nanoparticles into the ZnO thin films improves performance by enhancing the

[a]*Department of Physics, Rajdhani College, University of Delhi, Delhi 110015, India. E-mail: jasvirdalal2012@gmail.com*
[b]*Department of Physics, Hindu College, University of Delhi, Delhi 110007, India*
[c]*Department of Physics, Hansraj College, University of Delhi, Delhi 110007, India*
[d]*Department of Chemistry, Rajdhani College, University of Delhi, Delhi 110015, India*

photoinduced charge separation and reducing recombination losses, thereby boosting the photocurrent.[32,33] This modification leverages the favorable electron transfer dynamics between Au and ZnO and the plasmonic enhancement effects, which collectively allow for higher responsivity and detection ability in UV photodetectors.[25] Additionally, Au-modified ZnO devices show promise for flexible, wearable, and highly sensitive optoelectronic applications due to their improved stability and tunable spectral response.[33,34]

Previous studies recognized that post-deposition annealing temperature and detection layer thickness critically affect the physical and electrical properties of sol–gel-derived ZnO thin films.[35] Optimizing a 221 nm ZnO film annealed at 575 °C tailored its structure for UV sensing. However, higher dark current and limited I_{on}/I_{off} ratio restrict practical applications. Incorporating metals, especially Au, has shown promise for suppressing dark current *via* Schottky barrier formation while enhancing photocurrent through plasmon–exciton interactions.[36] Unlike prior works focused on higher-intensity UV (>mW cm^{-2}) with incomplete performance analyses, this study systematically evaluates Au–ZnO photodetectors under lower-intensity 24 μW cm^{-2} UV.[37,38] The optimized devices determine ultra-lower dark current (~nA), significantly enhanced photocurrent (mA scale) at 365 nm with 5 V bias, and the highest photoresponse gain (K) reported for sol–gel ZnO systems, outperforming literature benchmarks summarized in Table S1. The cost-effective sol–gel spin-coating combined with Au sputtering provides a scalable platform for higher-performance, lower-intensity UV detection. This work pioneers plasmonic Au overlayer optimization for ZnO UV photodetectors, evaluating physical, optical, electrical, and photoresponse properties systematically for the first time as per our nest knowledge.

2. Experimental details

2.1. Preparation of UV photodetector

ZnO and Au-overlayer/ZnO UV photodetectors were fabricated on Pt interdigital electrodes (IDEs) patterned on corning glass substrates using standard photolithography (Scheme 1). ZnO thin films were prepared through the spin-coating method using a ZnO solution prepared *via* sol–gel process. A 0.227 M zinc acetate dihydrate solution in methanol, stabilized with monoethanolamine (MEA) in a 1 : 1 molar ratio, was spin coated at 3000 rpm, followed by pyrolysis at 300 °C for 5 min after each coating. The films were subsequently annealed at 575 °C for 1 h to improve crystallinity. Before the spin coating; the corning glass substrates were cleaned by ultrasonic agitation in acetone, and deionized water for 10 minutes each to remove organic and particulate contaminants. This multistep cleaning ensures uniform film adhesion and reproducibility. Au overlayers of varying thicknesses (5–40 nm) were deposited by RF sputtering (sputtering rate ~0.16 nm s^{-1}, 99.9% pure Au target, 0.0027 kPa Ar pressure, 10 W power, 4 cm target-substrate distance). Post deposition annealing was carried out at 400 °C for 2 h in oxygen. For patterned Au deposition, a mesh with 200 μm pores was used during sputtering. Structural and optical properties of the films were characterized, while electrical and UV photoresponse measurements were performed on devices fabricated on the corning glass substrates. The ZnO thickness was fixed at its optimized value of 221 nm for maximum efficiency.[35] The effect of Au overlayer thickness on photoresponse parameters (I_{off}, I_{on}, gain, rise time, and fall time) was systematically examined and correlated with the structural and optical results.

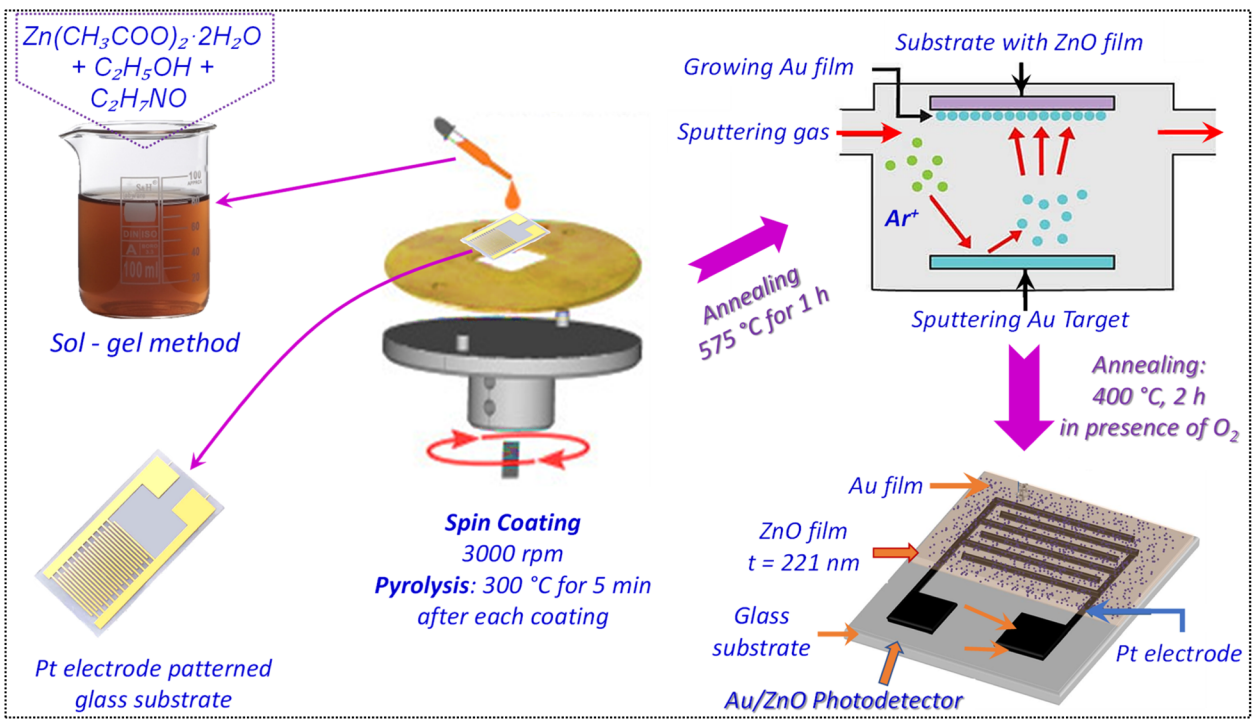

Scheme 1 Systematic presentation of process of preparation of UV photodetector.

2.2. Characterization techniques

The ZnO films were characterized for their physical and optical properties using Bruker D8 Discover X-ray diffraction system and Perkin Elmer lambda 35 UV-visible spectrophotometer respectively. Measurements of thickness were taken using Veeco Dektak 150 surface profiler having a vertical resolution of 2 nm. Scanning electron microscopy (SEM) has been done using Quanta 200 FEG SEM system. Steady-state UV photoresponse of the deposited ZnO films of varying thickness was recorded by illuminating the samples with 365 nm radiation (intensity of 24 μW cm^{-2}). The intensity of UV radiations was measured using a Newport optical power meter (model no. 1830 C). The semiconductor characterization system Keithley 4200 was used to acquire the photoresponse transients.

3. Results and discussion

3.1. X-ray diffraction studies

The XRD patterns of pure ZnO and Au-overlayer/ZnO thin films with Au thicknesses varying from 5 to 40 nm are shown in Fig. 1. The patterns show that all deposited thin films exhibit peaks corresponding to the hexagonal wurtzite structure of ZnO, confirming the growth of polycrystalline thin films.[39] The (002) diffraction peak is found to be significant, while the (100) and (101) peaks are relatively weak, indicating that the films are preferentially oriented along the (002) plane with the *c*-axis normal to the substrate. With the deposition of continuous Au overlayers, the diffraction peak corresponding to the (101) plane becomes dominant over the (002) and (100) peaks, as observed from Fig. 1. In addition, an intense peak at $2\theta \approx 38°$, corresponding to the Au (111) plane, is observed, confirming the presence of Au on the ZnO thin film surface.[23] The relative intensity of the Au (111) peak (I_{111}), calculated using the formula described in 35, increases continuously with Au overlayer thickness. This increase is attributed to the increase in number of Au atoms (act as diffracting centre) present on the ZnO surface with increasing thickness. Furthermore, an additional peak at ~44.5° is observed in all Au-overlayer/ZnO films. This peak can be assigned to the (440) diffraction plane of Au_2O_3, indicating the formation of gold oxide due to post-annealing of the films in an oxygen atmosphere. These oxygen vacancies produced additional electronic states in the forbidden gap of ZnO lattice and increased with the number of Au atoms. However, this peak may also correspond to the Au (200) reflection, generally located at ~44.3°, further supporting the presence of Au on the ZnO surface.

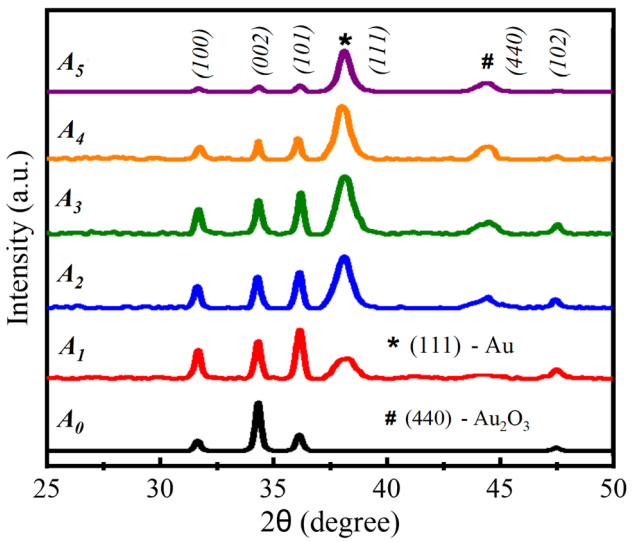

Fig. 1 XRD spectra of pure ZnO thin film and Au overlayer/ZnO films with Au thickness varying from 5 nm to 40 nm.

The structural parameters estimated from the XRD patterns are summarized in Table 1. These parameters are calculated on account of two significant peaks w.r.t. (002) & (101) planes using the Debye–Scherrer formula.[40,41] For the pure ZnO thin film (221 nm), the crystallite size was calculated to be 27 nm. With the deposition of Au, the crystallite size initially decreased to 23–24 nm for 5–10 nm Au thickness, indicating slight lattice distortion and strain at the ZnO surface due to Au incorporation. At intermediate thicknesses (20–30 nm), the crystallite size increased to 26–29 nm, suggesting partial grain coalescence and improved crystallinity. However, for the thickest overlayer (40 nm), the size decreased again to 26 nm, possibly due to increased scattering from Au agglomerates and the formation of Au_2O_3. The relative intensity of the Au (111) reflection (I_{111}) increased consistently with Au thickness, confirming progressive Au deposition. Also, the (440) reflection associated with Au_2O_3 became more pronounced, consistent with oxide formation during post-annealing in oxygen.

The Bragg angle shows a slight shift from 36.28° to 36.46° with increasing Au thickness, indicating minor lattice strain in ZnO. The variation in crystallite size and strain is observed from

Table 1 Various parameters calculated for pure ZnO (221 nm) and Au overlayer/ZnO thin films of varying Au thickness from 5 nm to 40 nm from XRD analysis

Thickness of Au overlayer (nm)	Relative intensity (I_{111})	Relative intensity (I_{440})	Bragg's angle ($2\theta°$)	FWHM	Crystallite size (nm)
0	—	—	34.36	0.309	27
5	0.17	0.03	36.28	0.37	23
10	0.50	0.07	36.30	0.351	24
20	0.51	0.08	36.32	0.319	26
30	0.82	0.11	36.38	0.289	29
40	1.71	0.13	36.46	0.323	26

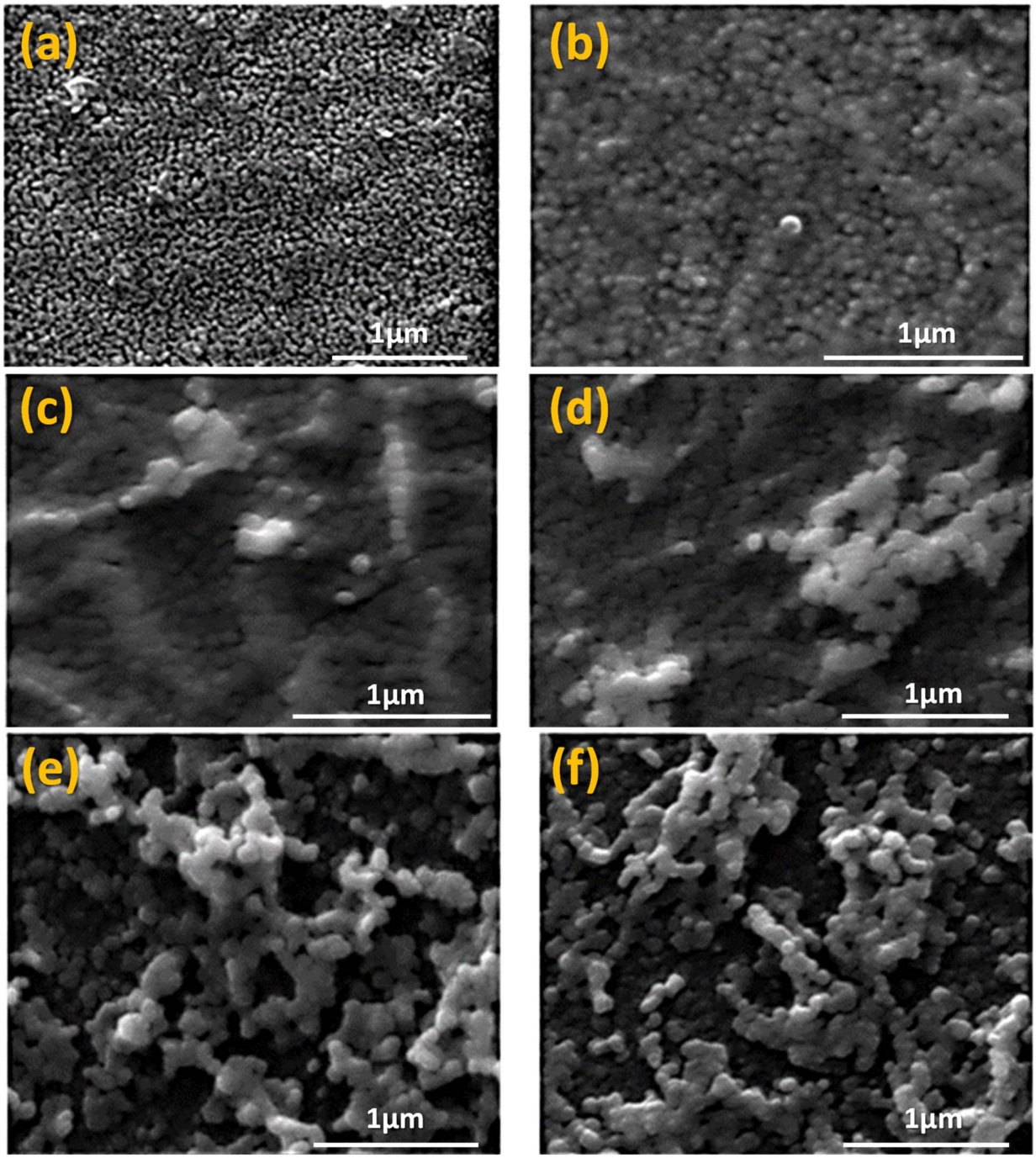

Fig. 2 Surface microstructure of (a) pure ZnO thin film and (b–f) Au overlayer/ZnO thin films having Au thicknesses: 5 nm, 10 nm, 20 nm, 30 nm and 40 nm, respectively. Scale is 1 μm.

variation in FWHM values; which signify the combined effects of both these parameters. Thus, the results confirm that Au overlayers affect the structural characteristics of ZnO thin films through the formation of Au_2O_3, along with modest changes in crystallite size and strain.

3.2. SEM analysis

SEM micrographs of pure ZnO and Au overlayer/ZnO thin films with varying Au thickness are presented in Fig. 2. The pure ZnO film (Fig. 2a) exhibits a dense and uniform surface morphology composed of nanosized grains, consistent with the crystallite sizes calculated from XRD. Upon deposition of Au, the surface features change markedly. At 5 nm, small bright granules, attributed to Au nanoparticles, are sparsely distributed across the ZnO surface, indicating isolated nucleation sites. With increasing thickness to 10 nm and 20 nm, the Au granules grow in size and density, beginning to coalesce into larger clusters. At higher Au thicknesses (Fig. 2e and f), the Au nanoparticles

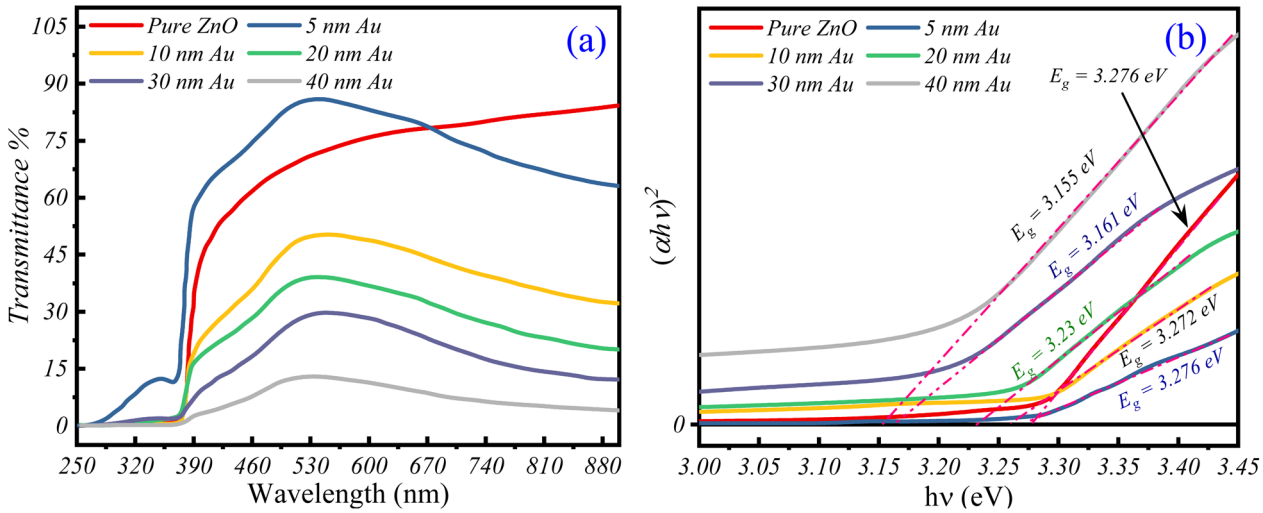

Fig. 3 (a) Optical transmittance spectra of pure ZnO thin film and Au overlayer/ZnO thin films with varying Au thickness. (b) Tauc plots used to determine the optical band gap of the thin films.

agglomerate significantly, forming large, interconnected clusters that progressively cover the underlying ZnO grains. The continuity of the Au overlayer is more pronounced at 40 nm, where most ZnO surface sites appear masked by the metallic layer. This morphological evolution reveals that Au growth progresses from isolated nanoparticles *i.e.*, island-like growth, at low thickness to nearly continuous overlayers at higher thickness, in agreement with the changes in crystallite size and strain observed in XRD.

This morphological growth is critical for UV photoresponse. At lower Au thicknesses (5–10 nm), isolated Au nanoparticles act as plasmonic hot spots, enhancing light absorption and exciton plasmon coupling while maintaining sufficient surface exposure of ZnO for oxygen adsorption–desorption. At intermediate thicknesses (20–30 nm), partial coalescence improves carrier transport by forming conductive pathways, while still retaining plasmonic enhancement. However, at higher thickness (40 nm), the nearly continuous Au film suppresses surface activity of ZnO and can increases dark current. Therefore, SEM analysis confirms that Au thickness directly influences the plasmonic enhancement and oxygen-mediated surface interactions, which govern the overall UV photodetector performance.

3.3. UV-visible spectroscopy

The UV-visible transmittance spectra of pure ZnO and Au overlayer/ZnO thin films with Au thickness varying from 5 nm to 40 nm, deposited on Corning glass substrates, are presented in Fig. 3a. Pure ZnO thin film exhibits high optical transparency (~80%) in the visible region, with a sharp absorption edge near 380 nm.[42] Deposition of the Au overlayer leads to a systematic reduction in transmittance. As the Au thickness increases from 5 nm to 40 nm, transmittance decreases significantly, from ~80% to ~5%.

The optical band gap (E_g) of the thin films was determined using Tauc plots,[43] obtained by extrapolating the linear portion of $(\alpha h\nu)^2$ *versus* $h\nu$ curves (Fig. 3b). The variation in E_g with Au thickness is summarized in Fig. 4. A clear band gap narrowing is observed, from 3.276 eV for pure ZnO to 3.155 eV for the 40 nm Au overlayer/ZnO thin film. The narrowing of the ZnO bandgap upon Au overlayer deposition, primarily attributed to lattice strain and defect states such as oxygen vacancies (due to formation of Au_2O_3), leads to shifts in the band alignment at the Au–ZnO interface.[22] This results in a downward shift of both the conduction band minimum and valence band maximum, effectively reducing the Schottky barrier height. Consequently, the modified band alignment facilitates improved charge carrier injection and separation under UV illumination, enhancing photocurrent generation while maintaining low dark current. Thus, bandgap narrowing plays a crucial role in tuning the electronic properties and improving the overall photoresponse of the Au–ZnO photodetectors. The progressive reduction in band gap with increasing Au thickness confirms the strong influence of Au deposition on the optical properties of ZnO thin films.

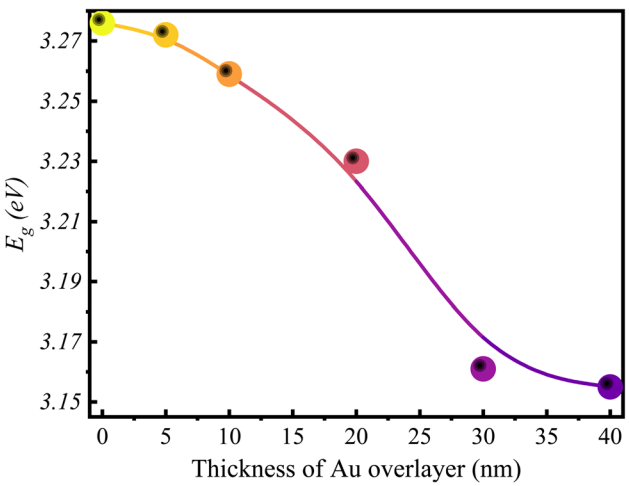

Fig. 4 Variation in optical band gap of pure ZnO and Au overlayer/ZnO thin films as a function of Au thickness.

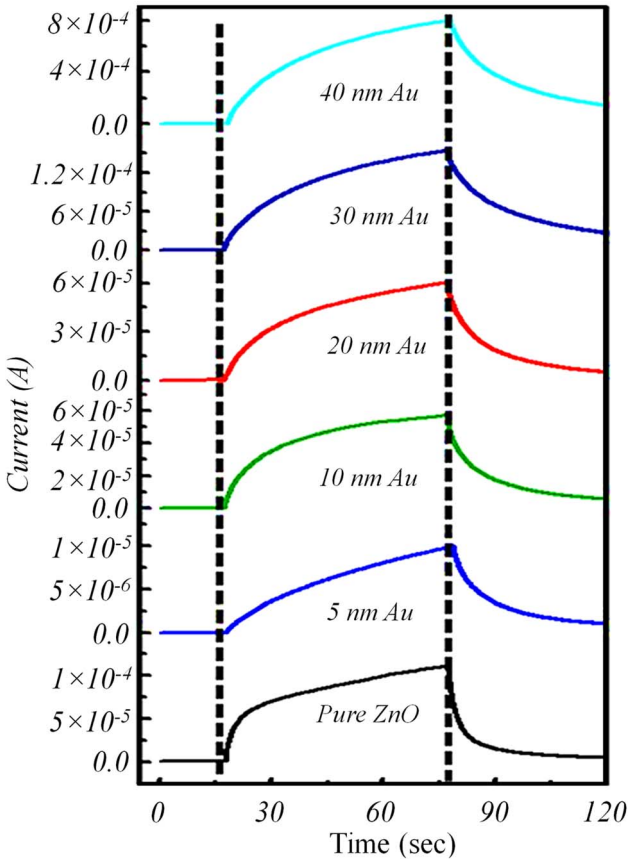

Fig. 5 Time-dependent on/off photoconduction measurements of pure ZnO and Au overlayer/ZnO thin film UV photodetector.

The optical findings are consistent with the XRD analysis, where the emergence and strengthening of the Au_2O_3 (440) diffraction peak with increasing Au thickness indicated oxide formation. Thus, both structural and optical analyses corroborate that Au_2O_3 formation, along with increasing Au coverage, governs the observed reduction in transparency and band gap narrowing.

Furthermore, these structural and optical modifications are expected to strongly influence the electrical transport and UV photoresponse behavior of the Au/ZnO photodetectors, which are analysed in the following section.

3.4. UV sensing response

The UV photoresponse characteristics of pure ZnO and Au overlayer/ZnO thin film-based photodetectors were investigated at a bias voltage of 5 V towards UV radiation of $\lambda = 365$ nm with an intensity of 24 μW cm^{-2}. Fig. 5 shows the time-dependent on/off photoconduction measurements of Au overlayer/ZnO thin film-based detectors.

For the 221 nm pure ZnO film, the dark current (I_{off}) is 0.73 μA, and the photocurrent (I_{on}) is 0.111 mA, nearly three orders of magnitude higher than the dark current. This UV response has already been reported[35] as the maximum among ZnO thin films of different thicknesses. Fig. 6a and b show the variation of I_{off} and I_{on}, respectively, with increasing Au overlayer thickness on the ZnO surface. Initially, I_{off} decreases drastically from 0.73 μA to 1.29 nA with the deposition of a 5 nm Au layer. However, with further increase in Au thickness (5–40 nm), I_{off} increases significantly, eventually reaching the μA range (Fig. 6a).

From Fig. 6a and Table 2, it is evident that dark current decreases sharply when a thin 5 nm Au layer is deposited, but increases progressively with further increase in Au thickness. The variation in dark current can be explained by three main factors: firstly, formation of Au–ZnO Schottky barrier at the interface; secondly, formation of Au_2O_3 phase, which increases oxygen vacancies and enhances I_{off}; and third is the availability of free ZnO sites, which adsorb oxygen and reduce I_{off}. The maximum suppression of dark current (1.29×10^{-9} A) occurs at 5 nm Au thickness. This reduction is attributed to the Schottky barrier formed at the Au–ZnO interface due to the higher work function of Au ($\phi_{Au} \approx 5.47$ eV) compared to ZnO ($\phi_{ZnO} \approx 4.45$ eV).[44,45] Scheme 2 shows the band alignment of isolated *n*-type ZnO and Au, Schottky barrier formation at the interface.

Under thermal equilibrium, electrons from the conduction band of ZnO transfer to Au, leading to downward band bending and the formation of a barrier potential (ϕ_B). This reduces dark

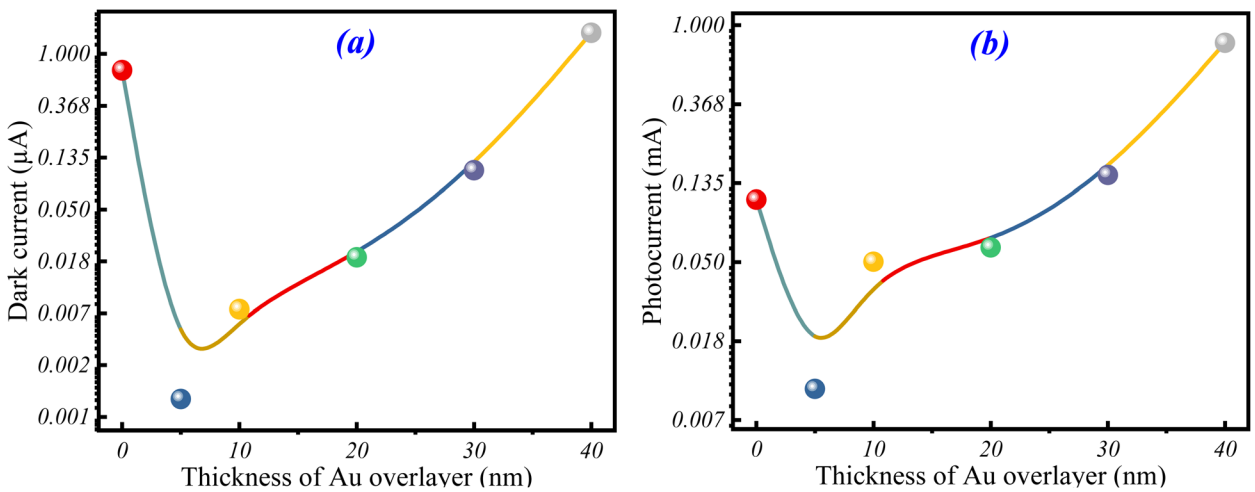

Fig. 6 (a) The variation in dark current (I_{off}) (b) and photocurrent (I_{on}) of the prepared UV photodetectors.

Table 2 UV photoresponse characteristics (dark current (I_{off}), photocurrent (I_{on}) and photoresponse (K), rise time (T_r) and fall time (T_f)) of pure ZnO thin film and Au overlayer/ZnO based UV photodetectors having different thickness of Au overlayer on ZnO surface

Thickness of Au	Dark current (I_{off}) (A)	Photocurrent (I_{on}) (A)	Photoresponse (K)	Rise time (T_r) (s)	Fall time (T_f) (s)
0	0.729×10^{-6}	0.11×10^{-3}	1.52×10^{2}	11.95	3.62
5	1.29×10^{-9}	0.01×10^{-3}	5.74×10^{3}	31.23	11.74
10	7.29×10^{-9}	0.05×10^{-3}	7.79×10^{3}	15.22	11.77
20	19.8×10^{-9}	0.06×10^{-3}	3.03×10^{3}	20.54	11.63
30	106×10^{-9}	0.15×10^{-3}	1.45×10^{3}	22.52	21.57
40	1.5×10^{-6}	0.80×10^{-3}	5.33×10^{2}	22.32	24.02

current since electron flow from Au atomic layer to ZnO conduction band is suppressed by the barrier $q\phi_B$. Moreover, SEM analysis confirms that the 5 nm Au film is not continuous, leaving ZnO surface sites available for oxygen adsorption, further lowering I_{off}. XRD results also support this, as the Au_2O_3 (440) peak shows the lowest intensity ($I_{440} = 0.03$) for 5 nm Au, indicating that factors (1) and (3) dominate over factor (2) as mentioned above. At higher Au thicknesses (10–40 nm), I_{off} increases significantly (up to 1.5 μA at 40 nm). This trend can be due to; enhanced formation of Au_2O_3, confirmed by the growing intensity of the (440) peak in XRD, leading to higher oxygen vacancy concentrations; in addition, improved continuity and coverage of the Au film, as seen in SEM, which reduces the number of ZnO sites available for oxygen adsorption. Thus, while the Schottky barrier should reduce I_{off}, oxygen vacancy formation and loss of adsorption sites dominate at higher thicknesses, leading to enhanced dark current.

On the other hand, the I_{on} also exhibits a thickness-dependent behavior as depicted in Fig. 6b. After deposition of 5 nm Au, I_{on} decreases drastically from 0.111 mA (ZnO) to 0.01 mA, likely due to a reduced number of oxygen vacancies. Although free ZnO sites are available for oxygen adsorption, the simultaneous reduction in vacancy-related defects lowers the net photocurrent. As Au thickness increases from 10 to 40 nm, I_{on} rises significantly, reaching 0.8 mA. This enhancement is attributed to: firstly, increased oxygen vacancies introduced by Au_2O_3 formation, which act as electron trap centers. Moreover, improved defect profile of the Au/ZnO system, facilitating higher carrier generation under UV illumination.

The photocurrent mechanism can be summarized as follows: oxygen vacancies act as trap centers for electrons, while adsorbed oxygen molecules capture conduction electrons, forming O_2^- species. Upon UV illumination, photogenerated holes neutralize trapped O_2^- ions, releasing electrons back to the conduction band, thereby increase in photocurrent.

The influence of Au overlayers on the photoresponse characteristics of ZnO-based UV photodetectors can be correlated with Schottky barrier modulation, oxygen vacancy concentration, and plasmonic effects. As shown in Fig. 7, the photoresponse (K) of pure ZnO (1.52×10^2) increases drastically to 5.74×10^3 upon deposition of a 5 nm Au layer, owing to the formation of a Schottky barrier at the Au/ZnO interface which suppresses the dark current and enhances the I_{on}/I_{off} ratio. A further increase to 10 nm thickness yields the maximum K value (7.79×10^3), attributed to the optimum balance between Schottky barrier height, limited Au_2O_3 formation, and plasmonic coupling effects that promote efficient carrier generation. At higher Au thicknesses (>10 nm), K decreases due to improved surface coverage by Au grains, which reduces the number of ZnO adsorption sites and increases oxygen vacancy

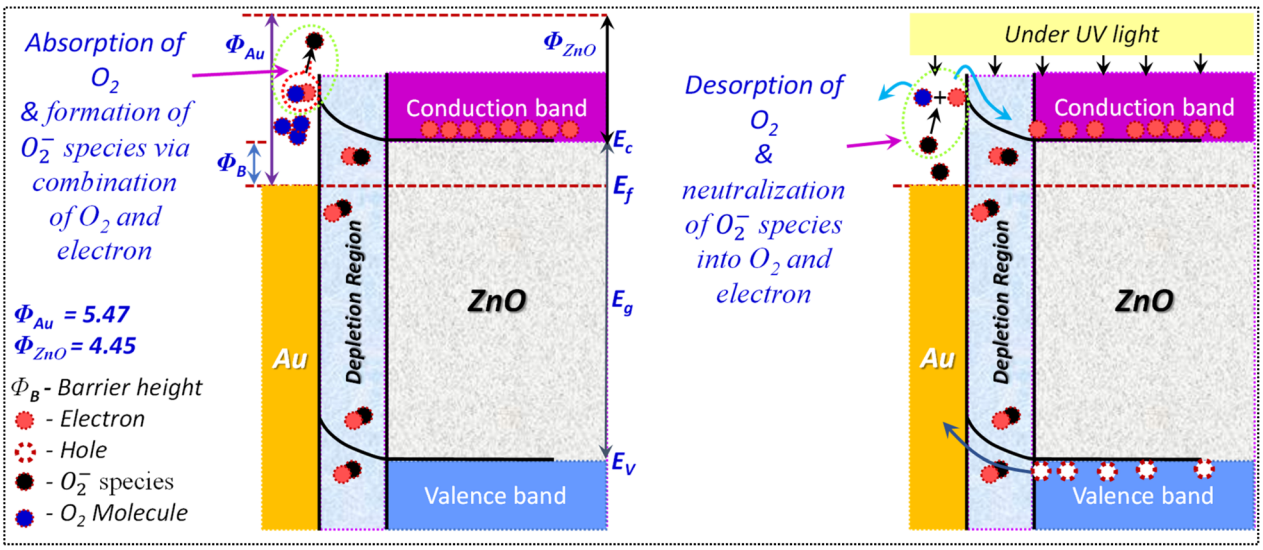

Scheme 2 Schematics energy band diagram of Au/ZnO and visualisation of photoresponse mechanism.

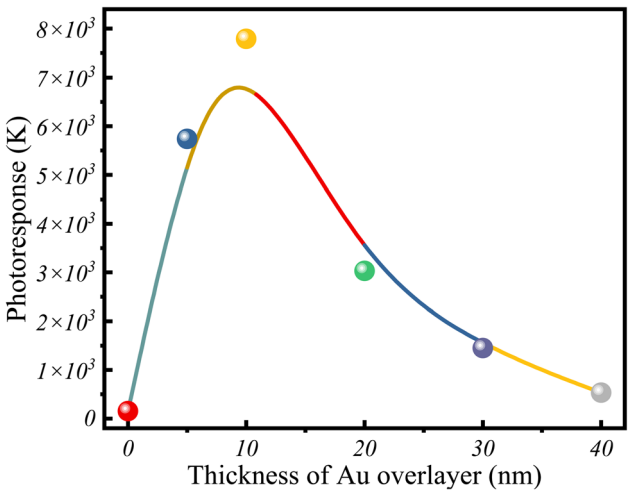

Fig. 7 Variation in photoresponse (*K*) of the prepared UV photodetectors.

defects through Au_2O_3 formation, thereby enhancing dark current. However, *K* remains significantly higher than that of pure ZnO.

The dynamic response parameters (Fig. 8) further highlight the role of Au overlayers in modulating charge transport and trapping. The rise time (T_r) increases to 31.23 s for 5 nm Au due to reduced oxygen vacancy concentration that slows down carrier release, but decreases to 15.22 s at 10 nm thickness as optimized defect density and plasmonic enhancement accelerate charge transport. For thicker overlayers, T_r again increases due to excessive oxygen vacancies acting as trapping centers. In contrast, the fall time (T_f) shows non-systematic variation with Au thickness, reflecting the complex interplay of recombination dynamics at defect states and the Au/ZnO interface. Thus, the integration of Au overlayers significantly enhances the photoresponse while offering tunable response times, with 10 nm Au providing the optimum balance of performance parameters.

From the figure it is observed that the T_r exceeds T_f at initial thickness, due to the oxygen-mediated photoconductivity mechanism dominant in ZnO: during UV "on", photogenerated holes must desorb surface O_2^- species (formed by pre-adsorbed O_2 capturing electrons), a process slowed by limited hole diffusion and Schottky barrier trapping at Au–ZnO interfaces; conversely, "off" recovery is faster as residual carriers recombine rapidly *via* defect states and plasmon-enhanced pathways. This $T_r > T_f$ trend is common in surface-controlled ZnO UV photodetectors, contrasting bulk-dominated devices, and Au modification balances it by optimizing defect density excess Au_2O_3 vacancies at >20 nm prolong both *via* trapping. Despite longer T_r, the devices achieve superior I_{on}/I_{off} (>7 × 10^3) at lower 24 μW cm^{-2}.

3.5. Photoresponse mechanism

The superior UV photoresponse of Au-overlayer ZnO photodetectors arises from synergistic oxygen-mediated photoconductivity, Schottky barrier effects, defect engineering, and plasmonic enhancement. The photoresponse mechanism can be summarized as follows: oxygen vacancies (Vo) act as trap centers for electrons, while adsorbed oxygen molecules capture conduction electrons, forming O_2^- species. Upon UV illumination, photogenerated holes neutralize trapped O_2^- ions, releasing electrons back to the conduction band, thereby increasing photocurrent. The whole mechanism is visualised in Scheme 2.

3.5.1. Dark current suppression (I_{off} mechanism). In ambient conditions, O_2 molecules adsorb on ZnO surface sites, capturing conduction band electrons to form O_2^- species and creating a low-conductivity electron-depleted layer. For pure ZnO, residual free carriers yield I_{off} = 0.73 μA. Au deposition (work function of Au = 5.47 eV > ϕ_{ZnO} = 4.45 eV) forms a Schottky barrier at the Au–ZnO interface, causing band bending and depleting electrons from ZnO near the interface (barrier height $q\phi_B \approx$ 0.5–1.0 eV). At 5–10 nm Au (island morphology), exposed ZnO maintains O_2 adsorption while

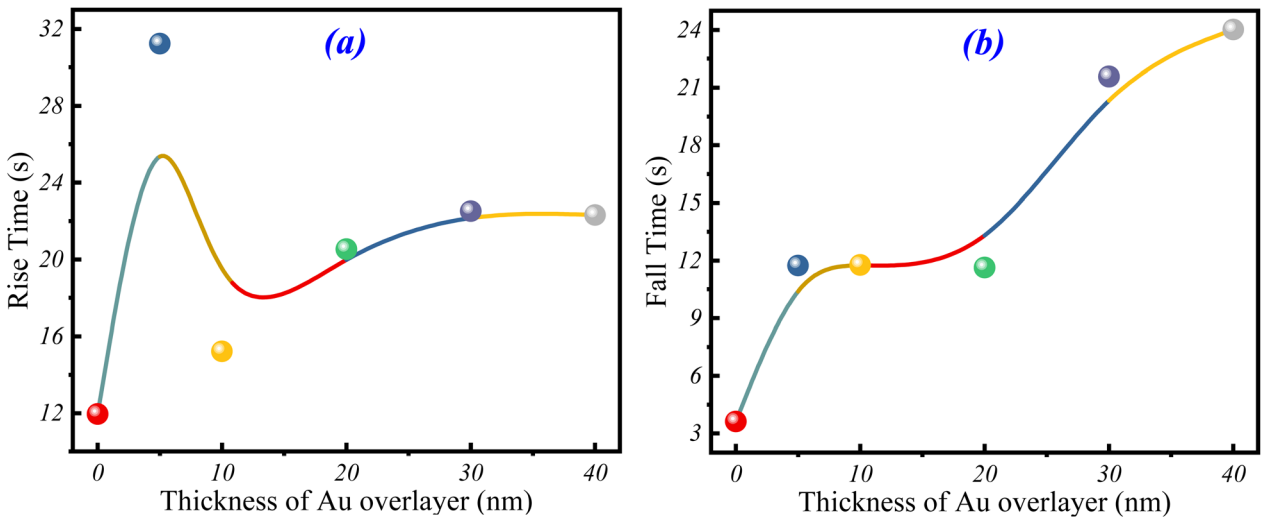

Fig. 8 Variation in (a) rise time (T_r) and (b) fall time (T_f) of the prepared UV photodetectors.

Schottky blocks carrier injection, yielding I_{off} = 1.29–7.29 nA. Thicker Au (>20 nm) forms continuous coverage more Au_2O_3, increasing oxygen vacancies (Vo^{2+}) that donate electrons, dominating to raise I_{off} to μA range.[44,45]

3.5.2. Photocurrent generation (I_{on} mechanism). Under 365 nm UV ($h\nu > E_g$ = 3.27 eV), electron–hole pairs generate across ZnO. Holes drift to surface, neutralizing $O_2^- \rightarrow O_2(g) + e^-(CB)$, collapsing depletion layer and releasing trapped Vo^{2+} electrons, yielding I_{on} surge (pure ZnO: 0.111 mA). Au overlayers modulate this: (1) plasmonic enhancement – Au nanoparticles (<20 nm) excite localized surface plasmon resonance (LSPR, Mie theory[36]), coupling UV photons to hot electrons that inject into ZnO CB *via* Schottky, boosting exciton generation ~2–5 times;[29,30] (2) Vo^{2+} traps – from Au_2O_3 amplify gain ($K = I_{on}/I_{off} = 7.79 \times 10^3$ max); (3) thicker Au increases I_{on} to 0.8 mA *via* vacancy proliferation despite coverage losses.

3.5.3. Dynamic response (T_r/T_f). $T_r > T_f$ reflects surface-dominated kinetics. UV-on requires sequential O_2^- neutralization and Vo^{2+} detrapping (slowed at 5 nm by lower Vo density); UV-off involves rapid e–h recombination *via* mid-gap states. Optimal 10 nm Au balances these (T_r = 15.22 s, T_f = 11.77 s).

This multi-mechanism synergy enables the Au/ZnO photodetector's ultra-sensitive detection at 24 μW cm^{-2}, showing its advantageous over the literature comprised in Table S1.

4. Conclusion

The integration of a gold thin film on ZnO surfaces significantly enhances the photoresponse characteristics of 221 nm ZnO thin film-based UV photodetectors. For the thickness of 10 nm Au overlayer results in substantial improvements in key parameters, including reduced I_{off}, increased I_{on}, and enhancement in the photoconductive gain (7.79×10^3) compared to the pure ZnO device (1.52×10^2). This improvement is attributed to the simultaneous suppression of dark current and enhancement of photocurrent, leading to superior photoresponse in the Au/ZnO hybrid system. However, increasing the Au overlayer thickness beyond 10 nm leads to performance degradation due to elevated dark current. Interestingly, while the Au thin film improves photoresponse, it also induces slower response and recovery times in the devices. These findings highlight that the higher work function of Au effectively reduces dark current, while the plasmonic effects of Au nanoparticles enhance optical absorption, collectively boosting the performance of ZnO-based UV photodetectors. Therefore, this study reveals the critical role of Au film thickness in tailoring the balance between dark current suppression and photocurrent enhancement, establishing Au-integrated ZnO thin films as promising candidates for high-performance UV photodetection.

Conflicts of interest

The authors declare that they have no known competing financial interests or personal relationships that could have appeared to influence the work reported in this paper.

Data availability

The data that support the findings of this study are available from the corresponding author up on reasonable request.

Supplementary information (SI) is available. See DOI: https://doi.org/10.1039/d5ra08186f.

References

1 H. K. Yadav, K. Sreenivas and V. Gupta, Persistent photoconductivity due to trapping of induced charges in Sn/ZnO thin film based UV photodetector, *Appl. Phys. Lett.*, 2010, **96**, 22.
2 L. J. Mandalapu, F. X. Xiu, Z. Yang and J. L. Liu, Ultraviolet photoconductive detectors based on Ga-doped ZnO films grown by molecular-beam epitaxy, *Solid-State Electron.*, 2007, **51**, 1014–1017.
3 N. Kouklin, Cu-doped ZnO nanowires for efficient and multispectral photodetection applications, *Adv. Mater.*, 2008, **20**, 2190–2194.
4 A. Kadir, X. Liu, F. Liu, T. Abdiryim, R. Jamal, N. Serkjan, X. Tang, Y. jun Liu and Y. Zhang, A self-powered UV photodetector from poly(3,4-ethylenedioxyselenophene)/Au nanoparticles-ZnO nanoarrays heterojunction, *Sens. Actuators, A*, 2023, **354**, 114308.
5 Y.-L. Chu, Y.-H. Liu, T.-T. Chu and S.-J. Young, Improved UV-Sensing of Au-Decorated ZnO Nanostructure MSM Photodetectors, *IEEE Sens. J.*, 2022, **22**, 5644–5650.
6 K. L. Foo, U. Hashim, C. H. Voon, M. Kashif and M. E. Ali, Au decorated ZnO thin film: application to DNA sensing, *Microsyst. Technol.*, 2016, **22**, 903–910.
7 W.-H. Liao, Y.-C. Yeh, Y.-L. Pan and C.-L. Hsu, High-sensitivity UV photodetector based on ZnO nanowires decorated with Au and $ZnAl_2O_4$ nanoparticles, *Ceram. Int.*, 2025, **51**, 9239–9247.
8 F. Cao and X. Ji, Enhanced self-powered UV sensing performance of ZnO/Au/Al_2O_3 photodetector with the decoration of Au nanoparticles, *J. Mater. Sci.: Mater. Electron.*, 2020, **31**, 2657–2665.
9 S. Rohilla, A. Gupta, V. Kumar, S. Kumari, M. Petru, N. Amor, M. T. Noman and J. Dalal, Excellent UV-light triggered photocatalytic performance of ZnO.SiO_2 nanocomposite for water pollutant compound methyl orange dye, *Nanomaterials*, 2021, **11**, 2548.
10 S. Gierałtowska, W. Zaleszczyk, M. Putkonen, D. Zasada, K. P. Korona and M. Norek, Regularly arranged ZnO/TiO_2, HfO_2, and ZrO_2 core/shell hybrid nanostructures-towards selection of the optimal shell material for efficient ZnO-based UV light emitters, *Ceram. Int.*, 2023, **49**, 31679–31690.
11 M. Kim, J. Beak, S. Kim, W. S. Hwang, B. J. Cho and M. Shin, Impact of oxygen deficiency and shallow hole-traps on high-responsivity ZnO-based UV photodetectors, *Sens. Actuators, A*, 2024, **369**, 115160.
12 S. Kumari, S. Malik, S. Kumar, J. Dalal, S. Dahiya, A. Ohlan, R. Punia and A. S. Maan, Excellent photoelectrical properties of ZnO thin film based on ZnO/epoxy-resin ink for UV-light detectors, *AIP Conf. Proc.*, 2019, 120004.

13 R. Sharma, N. Saxena, N. Pandey, A. Dawar, S. Ojha, V. Chawla, R. Laishram, R. Krishna and O. P. Sinha, Mg-doped tailoring of zinc oxide for UV-photodetection application, *Opt. Mater.*, 2022, **125**, 112056.
14 Z.-Q. Xu, H. Deng, J. Xie, Y. Li and X.-T. Zu, Ultraviolet photoconductive detector based on Al doped ZnO films prepared by sol–gel method, *Appl. Surf. Sci.*, 2006, **253**, 476–479.
15 T. Ghosh and D. Basak, Highly enhanced ultraviolet photoresponse property in Cu-doped and Cu–Li co-doped ZnO films, *J. Phys. D: Appl. Phys.*, 2009, **42**, 145304.
16 S. S. Shinde and K. Y. Rajpure, High-performance UV detector based on Ga-doped zinc oxide thin films, *Appl. Surf. Sci.*, 2011, **257**, 9595–9599.
17 H. K. Yadav, K. Sreenivas and V. Gupta, Study of metal/ZnO based thin film ultraviolet photodetectors: the effect of induced charges on the dynamics of photoconductivity relaxation, *J. Appl. Phys.*, 2010, **107**, 044507.
18 S. Mohammadnejad, S. G. Samani and E. Rahimi, Notice of Retraction: optical characteristics of ZnO—based photodetectors doped with Au nanoparticles, in *2010 2nd International Conference on Mechanical and Electronics Engineering*, 2010, p. V2-408.
19 K. W. Liu, B. Liu, S. J. Wang, Z. P. Wei, T. Wu, C. X. Cong, Z. X. Shen, X. W. Sun and H. D. Sun, Influence of thin metal nanolayers on the photodetective properties of ZnO thin films, *J. Appl. Phys.*, 2009, **106**, 083110.
20 S. Dhara and P. K. Giri, On the origin of enhanced photoconduction and photoluminescence from Au and Ti nanoparticles decorated aligned ZnO nanowire heterostructures, *J. Appl. Phys.*, 2011, **110**, 124317.
21 J. Sun, F.-J. Liu, H.-Q. Huang, J.-W. Zhao, Z.-F. Hu, X.-Q. Zhang and Y.-S. Wang, Fast response ultraviolet photoconductive detectors based on Ga-doped ZnO films grown by radio-frequency magnetron sputtering, *Appl. Surf. Sci.*, 2010, **257**, 921–924.
22 Z. S. Hosseini, H. A. Bafrani, A. Naseri and A. Z. Moshfegh, High-performance UV-Vis-NIR photodetectors based on plasmonic effect in Au nanoparticles/ZnO nanofibers, *Appl. Surf. Sci.*, 2019, **483**, 1110–1117.
23 M. R. Sekhar, R. Laha and M. Kar, Tuning optical and optoelectronic properties of gold nanoparticle and ZnO thin film hetero-structures, *Nano Express*, 2020, **1**, 30037.
24 H. Lee, J. H. Mun, I. Oh, K. Beom, T.-S. Yoon, A.-R. Hong, H. S. Jang and D. H. Kim, Enhanced photodetector performance in gold nanoparticle decorated ZnO microrods, *Mater. Charact.*, 2021, **171**, 110813.
25 W. Song, X. Dai, Y. He and T. Li, The Gold Nanoparticles Enhanced ZnO/GaN UV Detector, *IEEE J. Electron Devices Soc.*, 2022, **10**, 847–853.
26 M. Dagar, S. Kumar, A. Jain, A. Vohra, M. Singh, J. Dalal, S. Kumar and S. Kaushal, Synergistic Ce/Ag/N-doped ZnO–MWCNT nanocomposites for efficient photocatalytic wastewater remediation with visible light, *Mater. Adv.*, 2025, **6**, 4522–4537.
27 T. Han, Y. Xu, M. Shou, Z. Xie, L. Ying, C. Jiang, H. Wang, S. Ding, G. Jin, Q. Liu, *et al.*, Energy level gradient trapping based on different work functions of ZnO enhancing response and stablity for lateral photodetectors, *Org. Electron.*, 2020, **86**, 105883.
28 Y.-L. Chu, S.-J. Young, Y.-J. Chu, Y.-H. Liu and T.-T. Chu, High-performance UV photodetectors based on 1-D Ag/ZnO nanostructures with a simple photochemical process at room temperature, *IEEE Electron Device Lett.*, 2022, **44**, 124–127.
29 J. Zhang, X. Zhang, J. Li, Z. Ma, B. Leng, Q. Xia, L. Shen, Y. Song, Z. Fu, S. Feng, *et al.*, Simultaneous visible and ultraviolet photoresponse improvement of MoS_2/ZnO heterostructure photodetector *via* direct resonant coupling of Au nanoparticles localized surface plasmon resonance, *Opt. Mater.*, 2022, **124**, 111997.
30 H. Huang, J. Lai, J. Lu and Z. Li, Performance enhancement of ZnO ultraviolet detector by localized surface plasmon resonance of Al nanoparticles, *Appl. Phys. A*, 2021, **127**, 679.
31 E. Jeong, S.-G. Lee, J.-S. Bae, S. M. Yu, S. Z. Han, G.-H. Lee, E.-A. Choi and J. Yun, Effects of substantial atomic-oxygen migration across silver–oxide interfaces during silver growth, *Appl. Surf. Sci.*, 2021, **568**, 150927.
32 B. Deka Boruah, Zinc oxide ultraviolet photodetectors: rapid progress from conventional to self-powered photodetectors, *Nanoscale Adv*, 2019, **1**, 2059–2085.
33 S. Madhavanunni Rekha, H. Vadakke Neelamana and S. V. Bhat, Recent Advances in Solution-Processed Zinc Oxide Thin Films for Ultraviolet Photodetectors, *ACS Appl. Electron. Mater.*, 2023, **5**, 4051–4066.
34 S. Podder, B. Basumatary, D. Gogoi, J. Bora and A. R. Pal, Pyro-phototronic application in the Au/ZnO interface for the fabrication of a highly responsive ultrafast UV photodetector, *Appl. Surf. Sci.*, 2021, **537**, 147893.
35 A. Rajan, V. Gupta and K. Arora, Thickness dependent ultraviolet photoconductivity studies on sol–gel derived zinc oxide (ZnO) films, *Mater. Today Commun.*, 2023, **35**, 105507.
36 H. R. Stuart and D. G. Hall, Island size effects in nanoparticle-enhanced photodetectors, *Appl. Phys. Lett.*, 1998, **73**, 3815–3817.
37 X. Fei, D. Jiang, N. Wang, H. Zhao, M. Xing and H. Li, Study on Ultraviolet Photodetector modified by Au Nanoparticles on ZnO Nanowires, *J. Phys.: Conf. Ser.*, 2021, **1907**, 12044.
38 S. M. Abed, S. M. Mohammad, Z. Hassan, A. Muhammad, M. A. Ahmad and M. Syamsul, Fabrication of ultraviolet photodetector using Au nanoparticles decorated ZnO NRs/GaN, *Int. J. Nanotechnol.*, 2024, **21**, 236–250.
39 V. S. Rana, J. K. Rajput, T. K. Pathak and L. P. Purohit, Multilayer MgZnO/ZnO thin films for UV photodetectors, *J. Alloys Compd.*, 2018, **764**, 724–729.
40 H. Kaur, A. Sharma, K. Anand, A. Panday, S. Tagotra, S. Kakran, A. K. Singh, M. W. Alam, S. Kumar, G. Bouzid, *et al.*, Green synthesis of ZnO nanoparticles using *E. cardamomum* and zinc nitrate precursor: a dual-functional material for water purification and antibacterial applications, *RSC Adv.*, 2025, **15**, 16742–16765.
41 N. Kadian, R. Kumari, A. Panchal, J. Dalal and D. Padalia, Structural and Optical Properties of Gadolinium Doped-

Magnetite Nano-crystal for Photocatalytic Application, *J. Alloys Compd.*, 2023, **960**, 170811.

42 M. Mahajan, S. Kumar, J. Gaur, S. Kaushal, J. Dalal, G. Singh, M. Misra and D. S. Ahlawat, Green synthesis of ZnO nanoparticles using *Justicia adhatoda* for photocatalytic degradation of malachite green and reduction of 4-nitrophenol, *RSC Adv.*, 2025, **15**, 2958–2980.

43 P. Kumar, S. Kaushal, S. Kumar, J. Dalal, K. M. Batoo and D. S. Ahlawat, Recent advancements in pure and doped zinc oxide nanostructures for UV photodetectors application, *Phys. B: Condens. Matter*, 2025, 417177.

44 A. M. Lord, Q. M. Ramasse, D. M. Kepaptsoglou, P. Periwal, F. M. Ross and S. P. Wilks, Stability of Schottky and Ohmic Au nanocatalysts to ZnO nanowires, *Nano Lett.*, 2017, **17**, 6626–6636.

45 Z. Shao, H. Jia, Y. Zhang, X. Yang, M. Zhong and C. Chang, Oxygen Vacancy-Mediated Interfacial Charge Transfer of Au/ZnO Schottky Heterojunctions for Enhanced UV Photodegradation, *Int. J. Photoenergy*, 2020, **2020**, 2456968.